

## **Robots for machining tasks: stiffness simulation**

**Yair Shneur<sup>1</sup>, Vladimir Chapsky<sup>2</sup>**

<sup>1</sup>CAMT, Center for Advanced Manufacturing Technologies, Rotem Industries Ltd, Rotem Industrial Park, D.N. Arava ,Mishor Yamin , 86800, Israel, Phone: +972-8-6570692, Fax: + 972-8-6573365, e-mail: [yairshneur@gmail.com](mailto:yairshneur@gmail.com)

<sup>2</sup>Dept. of Mechanical Engineering, Ben-Gurion University of the Negev, Beer-Sheva, Israel, e-mail: [vchapsky@gmail.com](mailto:vchapsky@gmail.com)

### **1. Abstract**

**The use of industrial robots for machining applications can represent promising capabilities. Flexibility, cost effective, and versatility are among the advantages in comparison to machine tools. Due to the kinematics of the articulated robot, the system behavior is quite different compared to machine tool. The possibility of robot application for precise machining, and the influence of the stiffness of robot joints on the accuracy of the machined workpiece was investigated. A mathematical model of the robot structure and its stiffness developed, based on the Form-Shaping Function approach. The machining performances of the robot with focus on the achieve workpiece accuracy can be identified and evaluated using the developed model**

**Keywords: Robot stiffness, Form-Shaping function, Accuracy**

### **2. Introduction**

Early studies on robot machining were reported in the 1990s. Among the benefits in applying robots for machining tasks, we can define the increase of flexibility, as well as the lower cost. Robotic milling greatly increases the flexibility of milling compared to traditional machining centers. Robotic milling can be cheaper than CNC. Larger work piece volumes can be milled for a fraction of the cost of a large CNC machine. However, we have to be aware of the inherent weakness of industrial robots, that is, low positioning accuracy, vibration due to process force, and lack of reliable programming tool [3]. For articulated robots, the repeatability is inherently dependent on its reach distance. The larger the reach distance is, the lower the repeatability will be. Today's the repeatability of industrial articulated robot can be as high as  $\pm 0.01$  mm, which is sufficient for many low- to medium accuracy part machining jobs. The method presented in this paper enables us to simulate the robot positioning accuracy in milling process. The software developed particularly for vertical articulated robots, which have a significant distribution in the manufacturing industry [4].

### **3. Robot kinematic and stiffness model – Form-Shape Function**

This paper focused on modeling the robot-positioning errors associated with relatively low rigidity of the robot in comparison with CNC machines.

The investigations at CAMT were made with a 6 D.O.F robot type YASKAWA- MH12 (Fig.1).



Figure 1. Robot YASKAWA MH12

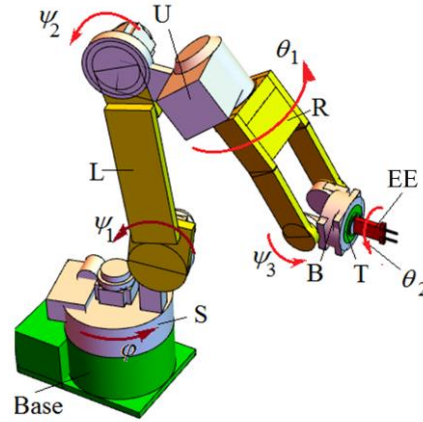


Figure 2. Kinematic model of the robot MH12

A mathematical model of the robot structure and its stiffness developed, based on the Form-Shaping Function (FSF) approach [3]. The FSF-based method presents an effective tool for the evaluation of geometric and kinematic errors. Errors analysis can be apply for the optimization of robot based machining processes in order to achieve specific accuracy.

### 3.1 Form-shaping function and manipulating matrix

The form-shaping system (*FSS*) of the machine tool or robot, presents an ordered aggregate of machine links, whose relative positions and mutual movements ensure the specified travel trajectory of a cutting tool (*CT*) with respect to a workpiece (*WP*).

FSF includes position and orientation components. The position component of the *FSF* connects two vectors  $\mathbf{r}_n$  and  $\mathbf{r}_0$  by means of the manipulating matrix  ${}^0\mathbf{A}_n$ .  $\mathbf{r}_n$ , position vector of functional point (*FP*), expressed in frame  $S_n$ ,  $\mathbf{r}_0$  - position vector of the same point, expressed in frame  $S_0$ .

$$\mathbf{r}_0 = {}^0\mathbf{A}_n \mathbf{r}_n \quad (1)$$

$$\mathbf{r}_0 = [x_0, y_0, z_0, 1] \text{ and } \mathbf{r}_n = [x_n, y_n, z_n, 1] \quad (2)$$

where  $x_0, y_0,$  and  $z_0$  are the coordinates of an *FP* referring to the frame  $S_0$ ;  $x_n, y_n,$  and  $z_n$  are those referring to the frame  $S_n$ ; and  ${}^0\mathbf{A}_n$  is the  $4 \times 4$  manipulating matrix of the *FSF* presenting a product of the cofactor-matrices  ${}^{i-1}\mathbf{A}_i$  associated with the  $i$ th link ( $i = 1, 2, \dots, n$ ) of the *FSS*,

$${}^0\mathbf{A}_n = \prod_{i=1}^n {}^{i-1}\mathbf{A}_i \quad (3)$$

$${}^{i-1}\mathbf{A}_i = {}^{i-1}\mathbf{A}_i(q_i), \text{ with } i \in 1, \dots, n \quad (4)$$

where  ${}^{i-1}\mathbf{A}_i$  is one of six matrices of elementary motions (translation along or rotation around the X-, Y-, or Z-axis);  $q_i$  is either a geometric constant (a constant length or a constant angle) associated with the  $i$ th geometric link or a time-dependent function,  $q_i = q_i(t)$ , for the 1-DOF kinematic link.

The orientation component of the *FSF* involves the same  $4 \times 4$  manipulating matrix  ${}^0\mathbf{A}_n$ , Eq. (3), and a pair of the  $4 \times 1$  non-position vectors  $\mathbf{c}_0$  and  $\mathbf{c}_n$ .  $\mathbf{c}_0$  - orientation vector, normal to the workpiece surface in the *FP*,  $\mathbf{c}_n$ , orientation vector along the *CT* axis to the *FP*.

**The 35th Israeli Conference on Mechanical Engineering – ICME 2018  
Beer-Sheva, 9-10 October 2018**

$$\mathbf{c}_0 = {}^0\mathbf{A}_n \mathbf{c}_n \quad (5)$$

With

$$\mathbf{c}_0 = [c_{0x}, c_{0y}, c_{0z}, 0] \text{ and } \mathbf{c}_n = [c_{nx}, c_{ny}, c_{nz}, 0] \quad (6)$$

where  $c_{0x}$ ,  $c_{0y}$ , and  $c_{0z}$  are the direction cosines referring to frame  $S_0$ ; and  $c_{nx}$ ,  $c_{ny}$ , and  $c_{nz}$  are those referring to frame  $S_n$ ; both  $\mathbf{c}_0$  and  $\mathbf{c}_n$  are the unit vectors,  $\|\mathbf{c}_0\| = \|\mathbf{c}_n\| = 1$ .

The *FSF* can combine both position and orientation components connecting by the same matrix. For example,

$$[\mathbf{r}_0 \ \mathbf{c}_0] = {}^0\mathbf{A}_n [\mathbf{r}_n \ \mathbf{c}_n] \quad (7)$$

### 3.2 Stiffness-Compliance analysis of serial robot

As shown in [2] the  $6 \times 6$  stiffness-compliance matrix of the terminal link of serial robot with respect to the base expressed through  $6 \times 6$  joint stiffness matrices as follows:

$$\mathbf{K}_{0N} = [(\mathbf{K}_{0,1})^{-1} + (\mathbf{K}_{1,2})^{-1} + \dots + (\mathbf{K}_{i-1,i})^{-1} + \dots + (\mathbf{K}_{N-1,N})^{-1}]^{-1} \text{ or } \mathbf{C}_{0N} = \sum_0^N \mathbf{C}_{i-1,i} \quad (8)$$

$$\mathbf{C}_{i-1,i} = (\mathbf{K}_{i-1,i})^{-1}$$

Where  $\mathbf{K}_{i-1,i}$  is the  $6 \times 6$  stiffness matrix of the  $i$ th link relative to its coordinate system, and

$\mathbf{C}_{i-1,i}$  is the  $6 \times 6$  compliance matrix of the same link. The problem is to represent all component of Eq. 8 in the same coordinate system.

Following equations gives the instrument to do it:

$$\mathbf{K}_{ij} = \mathbf{J}_{ij} \mathbf{K}_{\theta ij} (\mathbf{J}_{ij})^T, \mathbf{C}_{ij} = (\mathbf{J}_{ij} \mathbf{K}_{\theta ij} (\mathbf{J}_{ij})^T)^{-1} = (\mathbf{J}_{ij})^T \mathbf{C}_{\theta ij} \mathbf{J}_{ij} \quad (9)$$

Where  $\mathbf{K}_{ij}$  and  $\mathbf{C}_{ij}$  are the base-related stiffness and compliance of the joints respectively.

$\mathbf{K}_{\theta ij}$  and  $\mathbf{C}_{\theta ij}$  are diagonal matrices of the inner stiffness and compliance of the joints.

$\mathbf{J}_{ij}$  – the base-related Jacobian matrix of the joint.

If  $\mathbf{J}_i$  is joint-related Jacobian matrix consisting of Plucker coordinates of its supports, than:

$$\mathbf{J}_{ij} = {}^0\mathbf{T}_k \mathbf{J}_i \quad (10)$$

Where  ${}^0\mathbf{T}_k$  is the  $6 \times 6$  coordinate transformation matrix presenting a product of  $k$  elementary  $\mathbf{T}_j$  matrices ( $j=1, 2, \dots, 6$ ) defined as:

$${}^0\mathbf{T}_i = \prod_{k=0}^i {}^{k-1}\mathbf{T}_k \quad (11)$$

$$\mathbf{K}_{ij} = {}^0\mathbf{T}_k \mathbf{J}_i \mathbf{K}_{\theta ij} ({}^0\mathbf{T}_k \mathbf{J}_i)^T \quad (12)$$

$$\mathbf{C}_{i-1,i} = [({}^0\mathbf{T}_k \mathbf{J}_i) \mathbf{K}_{\theta ij} ({}^0\mathbf{T}_k \mathbf{J}_i)^T]^{-1} = [({}^0\mathbf{T}_k \mathbf{J}_i)^T]^{-1} \mathbf{C}_{\theta ij} ({}^0\mathbf{T}_k \mathbf{J}_i)^{-1} \quad (13)$$

The vector of tool tip deviation calculated as follows:

$$\mathbf{Vdev} = \mathbf{C}_{0N} \mathbf{Vforce} \quad (14)$$

where  $\mathbf{Vforce}$  is the  $6 \times 1$  vector of 3 linear forces and 3 angular moments acting on the tool tip.  $\mathbf{Vdev}$  is the  $6 \times 1$  vector of 3 linear and 3 rotational displacements of the tool tip.

## 4. The software developed

The presented software developed by using the symbolic computation system Wolfram Mathematica® [5]. The aims of the program is: (a) Calculate the compliance matrix of the robot terminal link with respect to the workpiece for all *FP*. (b) Estimate the deviation of the tip of cutting tool, from its nominal position, under the forces and moments during machining, due to

**The 35th Israeli Conference on Mechanical Engineering – ICME 2018  
Beer-Sheva, 9-10 October 2018**

robot joints elasticity. (c) Visualize the robot postures and position of robot links in machining of each *FP*.

Cutting tool deviations from its nominal position considered in two cases, taking into account the weights of robot links and without it. When the robot trajectory programming performed applying the teaching procedure of the relevant machining points the errors caused by links weight are already applied. If the machining trajectory programmed using *FP* coordinates in the previously defined user coordinate system, the weight of the links can affect the deviation of the cutting tool from the nominal trajectory points and should be calculate.

The visualization (Fig.3) includes the display of the compliance matrix, the angles of joints rotations, the vector of deviation and its components in the plain of workpiece and normal to this plain. The actual visualization of the robot postures corresponding to the processing at each function point.

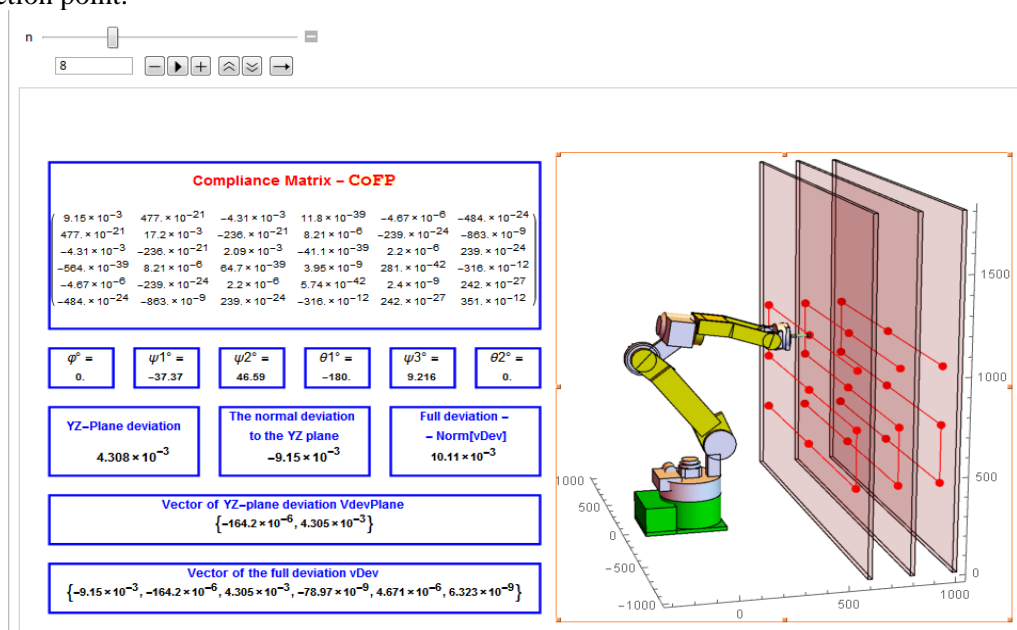


Figure 3. Visualization the moving of the robot, and results of calculations

## 5. Conclusions

The obtained values of the compliance matrix allow us to calculate and compose the ellipsoid of compliance and determine in advance the critical and optimal directions of the action of the machining forces. The proposed program allows determining the optimal mutual positioning of the robot and the workpiece, as well as the permissible processing parameters from the point of view of the effect of the stiffness of the robot joints. Further work will be focused on creating a robot simulation program taking into account the influence of link weight, as well as comparing the results of calculations with the errors of real processing.

## 6. References

- [1] Chen Y., Dong F., "Robot machining: recent development and future research issues", *Int J Adv Manuf Technol* (2013) 66:1489–1497.
- [2] Abele E., Weigold M., Rothenbücher S., "Modeling and Identification of an Industrial Robot for Machining Applications", *CIRP Ann.* 56/1/2007.
- [3] Portman, V., Inasaki, I., Sakakura, M., Iwatate, M., (1998), Form-shaping systems of machine tools: Theory and applications, *CIRP Annals - Manufacturing Technology*, 47/1, pp. 329-332,
- [4] Portman V. T., Shneur Y. , Chapsky V. S., Shapiro. A., "Form-shaping function theory expansion: stiffness model of multi-axis machines", *Int. J. Adv. Manuf. Technol.*, 76, pp. 1063-1078, 2015.
- [5] Wolfram Research, Inc., (2016) Mathematica, Version 10.0, Champaign, IL.